

# Identification of Mechanism of Action and Novel Compounds Targeting HsDHODH: Insights from Computational Analysis

Hengwei Bian<sup>1</sup>, Yalong Cong<sup>1</sup> and John Z.H., Zhang<sup>1-5\*</sup>

<sup>1</sup>*Shanghai Engineering Research Center of Molecular Therapeutics and New Drug Development, Shanghai Key Laboratory of Green Chemistry & Chemical Process, School of Chemistry and Molecular Engineering, East China Normal University at Shanghai, 200062, China*

<sup>2</sup>*CAS Key Laboratory of Quantitative Engineering Biology, Shenzhen Institute of Synthetic Biology, Shenzhen Institute of Advanced Technology, Chinese Academy of Sciences, Shenzhen, Guangdong, China*

<sup>3</sup>*NYU-ECNU Center for Computational Chemistry at NYU Shanghai, Shanghai 200062, China*

<sup>4</sup>*Department of Chemistry, New York University, NY, NY10003, USA*

<sup>5</sup>*Collaborative Innovation Center of Extreme Optics, Shanxi University, Taiyuan, Shanxi, 030006, China*

\*Corresponding authors: [John.zhang@nyu.edu](mailto:John.zhang@nyu.edu)

## **Abstract**

HsDHODH is a target of the human dehydrogenase enzyme, and HsDHODH inhibitors have shown potential applications in treating autoimmune diseases and cancer. Specific inhibitors have demonstrated potential therapeutic efficacy in treating autoimmune diseases like rheumatoid arthritis and systemic lupus erythematosus. However, the use of HsDHODH inhibitors may cause some side effects, such as interfering with DNA synthesis and causing apoptosis, which can be harmful to the body. In addition, drug resistance may occur during their use. Furthermore, the pharmacological mechanism of action of HsDHODH inhibitors is not fully understood, which may limit their use in treating specific diseases. Recently, the ASGBIE\_ESS method was used to calculate the binding free energy between HsDHODH and ascofuranone derivatives. The results showed a correlation of 0.9066 with experimental data, indicating the method's reliability. The energy decomposition analysis identified several hot-spot residues, including M13, L16, Q17, H26, F32, F68, R106, Y326, and T330, that play crucial roles in the ligand-protein binding process based on the crystal structure. Combining virtual screening with the ASGBIE\_ESS method, new compounds with unique backbones that have the potential to be valuable inhibitors of HsDHODH were identified. Remarkably, the computational predictions for the biological activity of these derivatives exceeded experimental results. The analysis showed that the identified compounds form stable hydrophobic interactions with residues around the pocket in the protein's hydrophobic region. Additionally, the binding ability of these derivatives is improved when they form hydrogen bonding interactions with specific residues in the pocket. In conclusion, this study provides valuable insights into the mechanism of ligand-protein binding for HsDHODH and offers promising leads for developing novel inhibitors targeting this enzyme.

Keywords: HsDHODH, ASGBIE, ESS, virtual screen, inhibitors

## 1.Introduction

Dihydroorotate dehydrogenase(DHODH) is an enzyme that contains iron and flavin and is located in the inner membrane of mitochondria. [1] Until now, DHODH becomes an attractive target for anti-malignance due primarily to its importance in tumorigenesis and metastasis. There are many canonical DHODH inhibitors have being reported, such as leflunomide,[2] BRQ,[3] teriflunomide,[4] ALASN003,[5] and BAY2202234.[6] However, the use of HsDHODH inhibitors may cause some side effects, such as interfering with DNA synthesis and causing apoptosis, which can be harmful to the body. In addition, drug resistance may occur during their use. Furthermore, the pharmacological mechanism of action of HsDHODH inhibitors is not fully understood, which may limit their use in treating specific diseases.[7, 8]Recently, ascofuranone(AF), a natural compound produced by *Acremonium sclerotigenum*, have been discovered by Miyazaki .et.[9] Additionally, they further discover a combination of compounds with excellent bioactivity and solve the crystal structure of them(Fig. 1).

Quantitative understanding of the different binding models of HsDHODH and inhibitors is essential to design novel selective HsDHODH inhibitors. However, the crystal structure of HsDHODH among AF and other compounds show very similar biding pose with a pocket RMSD of 5Å. Therefore, it is difficult to rationalize the selectivity based on the static crystal structures alone.

Computational simulation and accurate calculation of protein-ligand binding free energy is a powerful approach in understanding ligand binding mechanisms from a dynamic perspective.[10] Free energy perturbation(FEP) and thermodynamic integration(TI) are rigorous for binding free energy calculation, but there are not used routinely because of its high computational demand for such huge system.[11-15] On the contrary, the Molecular Mechanics/Generalized Born Surface Area (MM/GBSA) is a widely used method because of its efficiency in the absolute free energy calculation.[16-19] However, in this strategy, the entropy contribution is often neglected due to its high computational cost and rough accuracy.[20] Fortunately, Duan et al. has developed a method called interaction entropy(IE) for calculating entropy contribution which also perform well in other systems.[21, 22]

In general, although there are many residues around the pocket, only a few of them play the decisive role in protein-ligand binding.[23-26] Hence, to improve the binding potency and selectivity of ligand, we need to identify these hot-spot residues and explore the biding mechanism of protein-ligand. To this end, the alanine scanning (AS) approach has been combined with the MM/GBSA\_IE method to obtain binding free energy of specific residues.[27, 28] In this way, AS is carried out on each residue around the pocket in the trajectory after MD simulation which is performed starting from the initial complex structure; and then the enthalpy and entropic component are calculated with MM/GBSA and IE method.[29]

The discovery of new inhibitor molecules is urgent in the face of the strong side effects of inhibitors of HsDHODH and drug resistance. Virtual screening has become an effective method of drug discovery in the past years. Virtual screening has become a popular method for identifying potential inhibitors of DHODH. This computational

approach involves the use of software to screen large databases of chemical compounds and predict which ones are likely to bind to the target protein. Several virtual screening methods have been developed, including ligand-based and structure-based approaches. Structure-based methods, rely on the three-dimensional structure of DHODH to identify compounds that are predicted to bind to the protein's active site. These virtual screening method has been shown to be effective in identifying novel DHODH inhibitors, and several compounds identified using this approach have shown promising activity in preclinical studies.

In this study, We conducted molecular dynamics simulations on the crystal structures of the five HsDHODHs, using a sampling method we designed, and combined it with ASGBIE. Meanwhile, we analyzed the interaction of the five complex structures and identified the essential residue that serve as hot-spots for binding HsDHODH. Using this approach, we also performed virtual screening on this target and calculated the computational free energy while analyzing its interaction pattern.

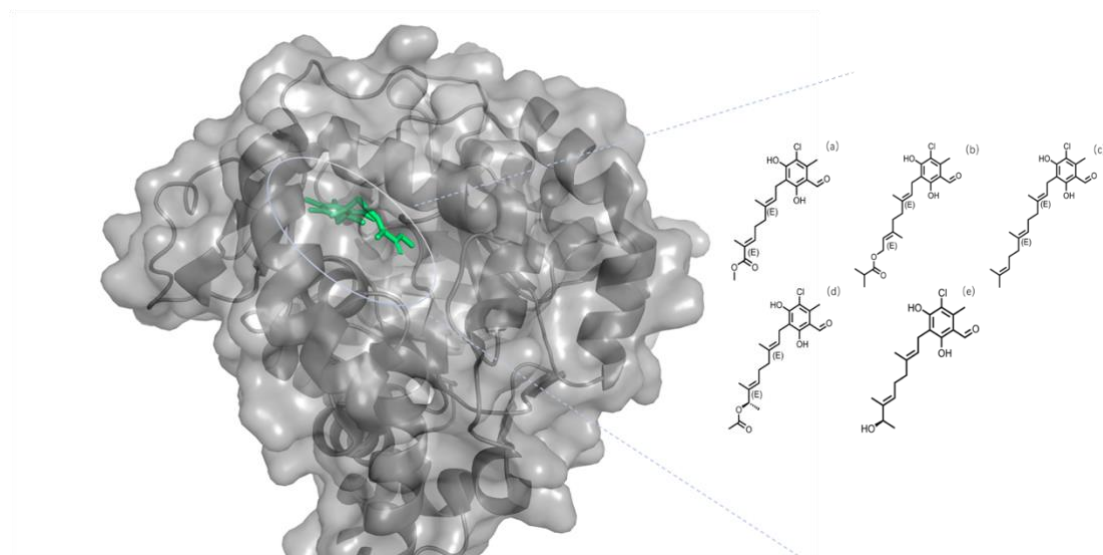


Fig1. Binding channels for the crystal structure of HsDHODH. (a) Ligand of 5ZF4 (b) Ligand of 5ZF9 (c) Ligand of 5ZF8 (d) Ligand of 5ZFA (e) Ligand of 5ZF7

## 2.METHOD

### 2.1MD Simulation

The five initial structures of HsDHODH (5ZF4, 5ZF7, 5ZF8, 5ZF9, 5ZFDA) were obtained from Protein Data Bank (<https://www.rcsb.org/>). The charge of the ligand was calculated using Proteins Plus.[30-32] Gaussian16 was used to obtain the parameter of the ligand. The force field utilized for the complex system was ff14SB, while GAFF was employed for the ligand. [33, 34] Counterbalance ions in the form of chloride and sodium were added to neutralize the system following the placement of the complexes into truncated octahedron TIP3P boxes, with a 12.0 Å buffer distance.[35] The conjugate gradient minimization method was employed, followed by the steepest descent method, to minimize the energy and eliminate any poor contact between solute and solvent water molecules. In the minimization process, the solvent water molecules are first optimized by constraining the coordinates of other molecules with a force constant of 500 kcal/(mol\*Å<sup>2</sup>). After minimizing, the system was heated to 300k within 300 ps from 0k with all solute atoms restrained with a force constant of 10 Kcal/(mol\*Å<sup>2</sup>). Next, the whole system was carried for 100 ns simulation in NPT ensemble with Langevin dynamics to maintain the temperature and Berendsen barostat to control the pressure in 1.0 atm.

### 2.2 MM/GB-SA

The MMGBSA (Molecular Mechanics/Generalized Born Surface Area) method is a widely used computational approach for calculating the binding free energy of biological macromolecules. The method combines the classical molecular mechanics force field (MM) and the GB/SA solvent model (Generalized Born/Surface Area) to simulate the structure and dynamics of biological macromolecules and calculate their interaction energies. The binding free energy is then computed by combining the solvation model and statistical thermodynamics methods. In the MMGBSA method, molecules are treated as a series of atoms, and their interaction energies can be calculated using classical force fields, which typically include bond energies, angle energies, and flexible bond energies. Meanwhile, the MMGBSA method also considers the interactions between molecules and the surrounding solvent, including surface tension and solvation energy. The MMGBSA method can be applied to study biological problems such as molecular binding, protein stability and conformational changes, and enzyme catalytic mechanisms. Its advantages include high computational efficiency, applicability to large molecules, and the ability to consider solvent effects.

The most basic principle of this method is to calculate the difference in energy before and after binding of the receptor and ligand, which can be expressed by the formula:

$$\Delta G_{bind}^0 = \Delta G_{complex}^0 - (\Delta G_{ligand}^0 + \Delta G_{receptor}^0) \quad (1)$$

In practical calculations, however, a serious problem is encountered - the energy contribution comes mainly from inter-solution interactions and the total energy fluctuates much more than the binding energy, so that it takes a very long time to converge. The total free energy of binding in the solvent is therefore split into the binding energy in vacuum and the solvent wah energy, which can be expressed as:

$$\Delta G_{bind,solv}^0 = \Delta G_{bind,vacuum}^0 + \Delta G_{bind,complex}^0 - (\Delta G_{solve,ligand}^0 + \Delta G_{solv,receptor}^0) \quad (2)$$

The method for calculating the free energy of binding in a vacuum is the same as the previous method for calculating the total free energy of binding, which can be expressed as:

$$\Delta G_{bind,vacuum}^0 = \Delta G_{complex,vacuum}^0 - (\Delta G_{ligand,vacuum}^0 + \Delta G_{receptor,vacuum}^0) \quad (3)$$

According to the definition of the free energy of binding, for each molecule, the following equation is used:

$$\Delta G_{vacuum}^0 = \Delta E_{MM}^0 - T\Delta S^0 = (\Delta E_{int}^0 + \Delta E_{ele}^0 + \Delta E_{vdw}^0) - T\Delta S^0 \quad (4)$$

$T\Delta S^0$  is the entropic contribution, which can be obtained by simple normal mode analysis. However, in practice, this contribution is usually ignored. Because systems calculated using the MMGBSA scheme usually have little conformational change before and after receptor-ligand binding, this contribution can be cancelled out in the calculation of the difference.

The solvation energy can be divided into two parts: polar solvation energy and non-polar solvation energy, which can be expressed as:

$$\Delta G_{solv}^0 = \Delta G_{sole,polar}^0 + \Delta G_{sole,nonpolar}^0 \quad (5)$$

For polar non-solventing energies there are two main methods: Poisson-Boltzmann (PB) and GeneralizedBorn (GB), The non-polar solvation energy can be expressed by the following equation:

$$\Delta G_{sole,nonpolar}^0 = \gamma SASA + \beta \quad (6)$$

Thus, for each term on the right-hand side of the equation in equation 1, it can be expressed as:

$$\Delta G^0 = \Delta G_{vdw}^0 + \Delta G_{ele}^0 + \Delta G_{solv,polar}^0 + \Delta G_{nonpolar}^0 \quad (7)$$

### 2.3 ASGBIE

In the recent years, Alanine scanning mutations have solved many computational problems as an important computational method in computational biology. Alanine, the simplest of the residues, has only one methyl group in its residue side chain. The size of its side chain is so small that it has no effect on the conformation of the side chain and has negligible effects on the structure and spatial and electrostatic effects of the protein. Using this method, the residues on the surface of the protein can be mutated to alanine, and the difference in free energy of binding before and after the mutation can be calculated to determine the importance of these residues in the binding process. The residue of interest is mutated to alanine, and the contribution of that residue to the binding free energy is determined by referencing the change in binding free energy

before and after the mutation, which is defined as:

$$\Delta\Delta G_{\text{bind}}^{x\rightarrow a} = \Delta G_{\text{bind}}^a - \Delta G_{\text{bind}}^x = \Delta\Delta G_{\text{gas}}^{x\rightarrow a} + \Delta\Delta G_{\text{sol}}^{x\rightarrow a} \quad (8)$$

$\Delta\Delta G_{\text{bind}}^{x\rightarrow a}$  is the contribution of this residue x to the free energy of binding.  $\Delta G_{\text{bind}}^x$  is the calculated free energy of binding of the protein to the ligand in the wild type.  $\Delta G_{\text{bind}}^a$  is the calculated binding free energy of the mutant with the ligand after the mutation of this residue to alanine. The calculation formula of free energy of gas phase and solvation is expressed as follows:

$$\Delta\Delta G_{\text{gas}}^{x\rightarrow a} = \Delta G_{\text{gas}}^a - \Delta G_{\text{gas}}^x \quad (9)$$

$$\Delta\Delta G_{\text{sol}}^{x\rightarrow a} = \Delta G_{\text{sol}}^a - \Delta G_{\text{sol}}^x \quad (10)$$

In the formula (9) and (10),  $\Delta G_{\text{gas}}^x$  represents the binding energy in the gas phase and  $\Delta G_{\text{sol}}^x$  represents the binding energy in the solvent phase. Same to formula (8), gas energy and solvent energy also calculate the free energy of binding before and after the mutation. Following this method, all residues in the vicinity of the binding pocket are mutated, and the contribution of each residue is calculated, and finally add these contributions to calculate the difference in energy before and after the mutation to the total binding free energy.  $\Delta G_{\text{gas}}^x$  is calculated by IE method:

$$\Delta G_{\text{gas}}^x = \langle E_{\text{int}}^x \rangle - T\Delta S_{\text{int}}^x = \langle E_{\text{int}}^x \rangle + KT \ln \langle e^{\beta\Delta E_{\text{int}}^x} \rangle \quad (11)$$

and likewise, for the alanine mutant:

$$\Delta G_{\text{gas}}^a = \langle E_{\text{int}}^a \rangle + KT \ln \langle e^{\beta\Delta E_{\text{int}}^a} \rangle \quad (12)$$

Here, the interaction energies of ligands with residues x and a are represented by  $E_{\text{int}}^x$  and  $E_{\text{int}}^a$ , respectively.

$$\langle e^{\beta\Delta E_{\text{int}}^x} \rangle = \frac{1}{N} \sum_{i=1}^N e^{\beta\Delta E_{\text{int}}^x(t_i)} \quad (13)$$

Where N is the number of MD snapshots. Therefore, equation (9) becomes:

$$\Delta\Delta G_{\text{gas}}^{x\rightarrow a} = \Delta\Delta E_{\text{gas}}^{x\rightarrow a} - T\Delta\Delta S_{\text{gas}}^{x\rightarrow a} = \langle E_{\text{int}}^a \rangle - \langle E_{\text{int}}^x \rangle + \left[ \ln \langle e^{\beta\Delta E_{\text{int}}^a} \rangle - \ln \langle e^{\beta\Delta E_{\text{int}}^x} \rangle \right] \quad (14)$$

The polarity term of the solvent wavenumber is calculated under the obc-gbsa model using IGB=2, where the dielectric constants of nonpolar, polar and charged residues are set to 1, 3 and 5, respectively. The total free energy of binding is calculated as the sum of the contributions of each residue within pocket 5Å:

$$\Delta G_{bind} = -\sum_x \Delta \Delta G_{bind}^{x \rightarrow a} \quad (15)$$

When calculating the entropy of the binding freedom, researchers in the past have often used the regular mode method to calculate the entropy of protein ligands. But the high cost of the calculation has been a deterrent. Recently, our group has developed a new method for calculating the entropy in the binding free energy, which is called interaction entropy. Compared to old methods, the process of this method is rigorous and efficient. Here, the interaction entropy (IE) is defined as:

$$-T\Delta S = KT \ln \left\langle e^{\beta \Delta E_{pl}^{int}} \right\rangle \quad (16)$$

#### 2.4 Energy Stable Simpling(ESS)

To address the issue of poor correlation between calculated and experimental results due to fluctuations in MD trajectories, a method is defined to identify a stable fragment of trajectory energy for the calculation of ASGBIE. The method involves the following steps:

First, calculate the energy of each frame using the formula:

$$\Delta E_{MM} = \Delta E_{ele} + \Delta E_{vdw} \quad (17)$$

where  $\Delta E_{ele}$  is the electrostatic interaction energy and  $\Delta E_{vdw}$  is the van der Waals interaction energy in the gas phase.

Then, The sample size needed to calculate based on the length of the trajectory and the desired level of accuracy can be determined. For each step  $i$ , calculate the root mean square deviation (RMS) of the energy over  $k$  frames using the formula:

$$RMS = \sqrt{\frac{\sum_i^{i+k-1} (\Delta E_{MM}(i) - \langle \Delta E_{MM} \rangle)^2}{k}} \quad (18)$$

where is  $\langle \Delta E_{MM} \rangle$  the average energy over the  $k$  frames centered on  $i$ . Finally, Select the section of the trajectory with the smallest RMS value.

$$RMS_{min} = \min(RMS) \quad (19)$$

#### 2.4 Virtual Screening

The HsDHODH protein used in this study was obtained from the RCSB database (PDBID: 5ZF4, resolution: 1.66 Å). To prepare the protein, the crystal structure was processed to remove water and other molecules, leaving only the protein and the active ligand. The protein structure was then hydrogenated and optimized at pH 7.4 using the OPLAS2005 force field. The docking box was positioned around the active molecule's geometric center, with a radius of 25 Å. A total of 250,000 ligands were obtained from SPECS (<https://specs.net/>). Before docking, the energy of each ligand was minimized using the OPLS 2005 force field. The ligands were generated in all of their ionized states at pH 7.4, resulting in a single, low-energy three-dimensional structure while preserving the original chiral state of each input structure. Finally, the SP model of Glide was utilized for docking scoring.[36]



## 3.RESULTS AND DISCUSSION

### 3.1 Stability of the Complex Systems

In molecular dynamics (MD) simulation, it is essential to ensure the stability of the complex system before performing energy calculations and analyzing the interaction mechanism. One of the crucial measures of stability is the root-mean-square deviation (RMSD). Therefore, we calculated the RMSD of protein backbones and small molecules in five systems, as shown in Figure S1. The RMSD of the ligands in 5ZFA, 5ZF8, 5ZF9, and 5ZF4 were stable around 1.5 Å, while the RMSD of the ligand in 5ZF7 had some fluctuations but was still within 2 Å of the average.

To evaluate the stability of protein-ligand binding, an analysis of the temperature anisotropy (B-factors) of the protein backbone was conducted and the results are presented in Figure 2. B-factors for the three trajectories of each system were calculated and compared to the experimental results. The observed movement trends are consistent with those of the B-factors obtained from the crystal structure, providing further evidence of the stability of the protein-ligand complex. Based on these findings, we can assume that the MD simulations for the five complex systems are reliable and can be used for subsequent energy calculations and interaction analysis.

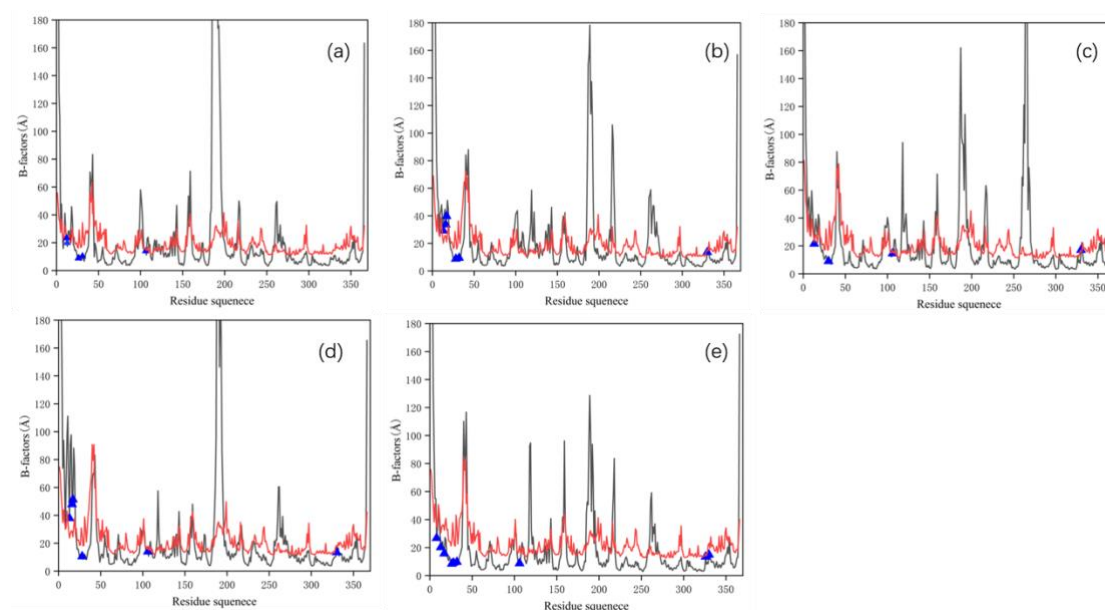


Fig2. B-factors of the protein backbone in the different complex. (a)The complex of 5ZF4; (b) The complex of 5ZF9; (c) The complex of 5ZF8; (d) The complex of 5ZFA; and (e) The complex of 5ZF7. Hot-spot residues are marked with blue triangles.

### 3.2 Analysis of calculation methods

Binding free energy is a crucial measure of a protein's ability to bind to a ligand. In this study, we utilized several approaches, as depicted in Fig. 2, to calculate the binding free energy of HsdHODH and ligands, which is used to characterize biological activity of the molecules

Initially, we utilized the conventional GB model (IGB2) to calculate MMGBSA for the

last 50 nanoseconds of molecular simulation. However, the correlation of calculated and experimental values is negative (-0.7918), as shown in Fig. 1, making its calculation impractical as a reference. Therefore, we added the method of alanine scanning, which increased the correlation between the calculated results and the experimental values to 0.5825 (Fig. 1). Detail result of binding free energy was shown in Table S1 of the Supporting Information.

We then tested the ASGB method with the addition of the interaction entropy (IE) method, which resulted in a correlation increase to 0.8372 (Fig. 3). Recently, a new GB model (IGB8) became available, and we evaluated its impact on the method. As shown in Fig 3, the traditional MMGBSA approach still exhibits a negative correlation. However, after incorporating an alanine scan and the IE method, the IGB = 8 model demonstrated improved correlation with experimental values compared to the previous model. Nonetheless, the correlation was still not as high as that of the traditional IGB2 model.

To further enhance the correlation between calculated results and experimental values, we proposed a new sampling method, ESS. We tested the results of adding this new sampling method under the IGB2 model, and the correlation significantly improved to 0.9066. Similarly, under the IGB8 model, this sampling method allowed for a better correlation between the calculated results and the experimental values, reaching 0.8423. Therefore, we believe that a method such as ASGBIE, combined with the ESS sampling method, provides more accurate results for the calculation of the binding free energy in HsDHODH-ligand system.

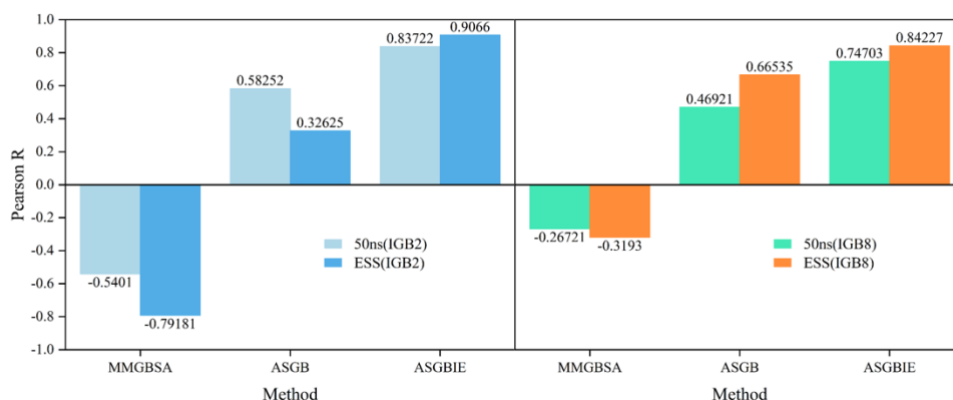


Fig2. Correlation of different calculated results with experimental values.

### 3.3 Residue-Specific Binding Free Energies

To better understand the variability in the binding capacity of the five inhibitors, we analyzed the contribution of the binding free energy of each residue within the binding pocket of 5Å. We identified residue that contribute greater than 1.5 kcal/mol as hot-spot residues and those that contribute greater than 1.0 kcal/mol as warm-spot residues. The three systems with better biological activity (5ZF4, 5ZF9, 5ZF8) had slightly fewer warm-spot residues and hot-spot residues than the less biologically active systems (5ZFA, 5ZF7).

While 5ZF4 and 5ZF7 have more hot and warm spots, they both have a negative contributing residue (GLU23) that forms an electrostatic repulsion with the ligand, leading to a negative contribution to the binding. In contrast, the three systems with better biological activity do not have many hot-spots and warm-spots in terms of quantity. However, since the binding pocket of human HsDHODH is a long channel, the number of residues contributing in the range of 0.8-1.0 kcal/mol is high in the three systems of 5ZF4, 5ZF9, and 5ZF8, which leads to their excellent biological activity. Overall, our analysis suggests that the major binding energy contributions of the less biologically active systems were due to individual residue contributions, whereas the binding pocket of the more active systems is characterized by a high number of residues contributing at a moderate level.

To analyze the primary binding mechanisms of each system, we aggregated the hot-spot residues for each one (as shown in Fig. 3). Among them, MET13 emerged as a major contributor due to its longer side chain and ability to form larger van der Waals interactions with the ligand. In contrast, charged residues such as GLN17 and ARG306 were found to form highly stable hydrogen bonds with their ligands (e.g., 5ZF7), suggesting that molecular designs should consider optimizing for these interactions as well. Moreover, our analysis revealed that LEU16 and THR330 make consistent contributions across all systems, and therefore, their interactions should also be considered during molecular design. Additionally, PHE32 and PHE68 were observed to form stable p- $\pi$  interactions with C atoms on the ligand due to their aromatic side chains, which could further enhance binding affinity. In summary, understanding the key hot-spot residues and their interactions with the ligand is crucial for designing more effective molecular structures. By taking into account the contributions of MET13, GLN17, ARG306, LEU16, THR330, PHE32, and PHE68, it may be possible to optimize the binding affinity of a given system and improve its overall performance.

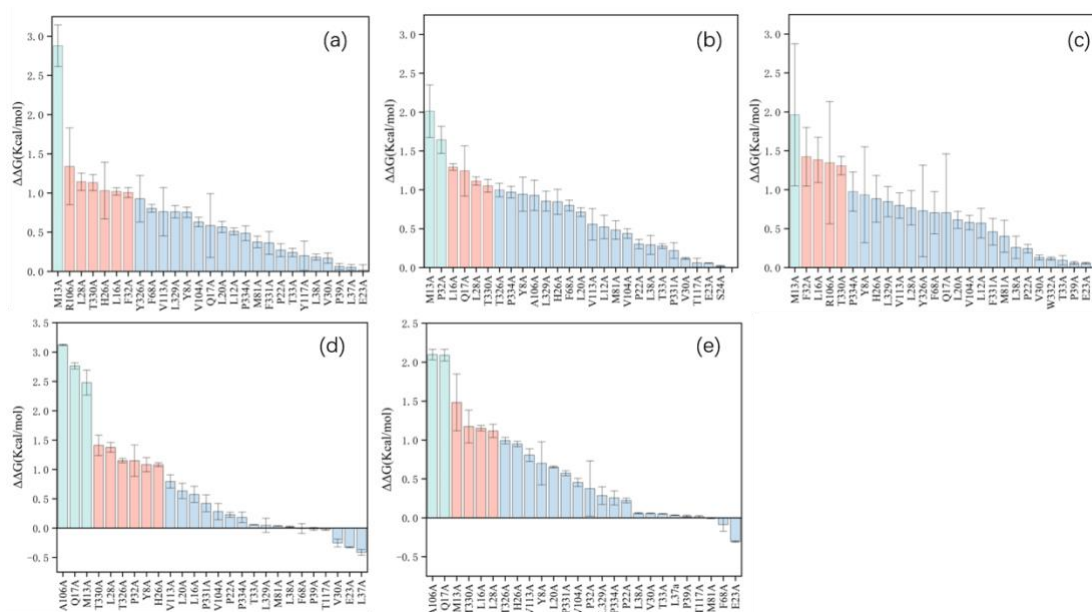


Fig4. The contribution of each residue to the binding free energy calculated by the ASGBIE\_ ESS method. (a) Complex of 5ZF4; (b) Complex of 5ZF9; (c) Complex of 5ZF8; (d) Complex of 5ZFA; (e) Complex of 5ZF7. Residues contributing more than

1.5kcal/mol are shown in cyan, residues contributing between 1 and 1.5kcal/mol are shown in orange and residues contributing less than 1kcal/mol are shown in blue.

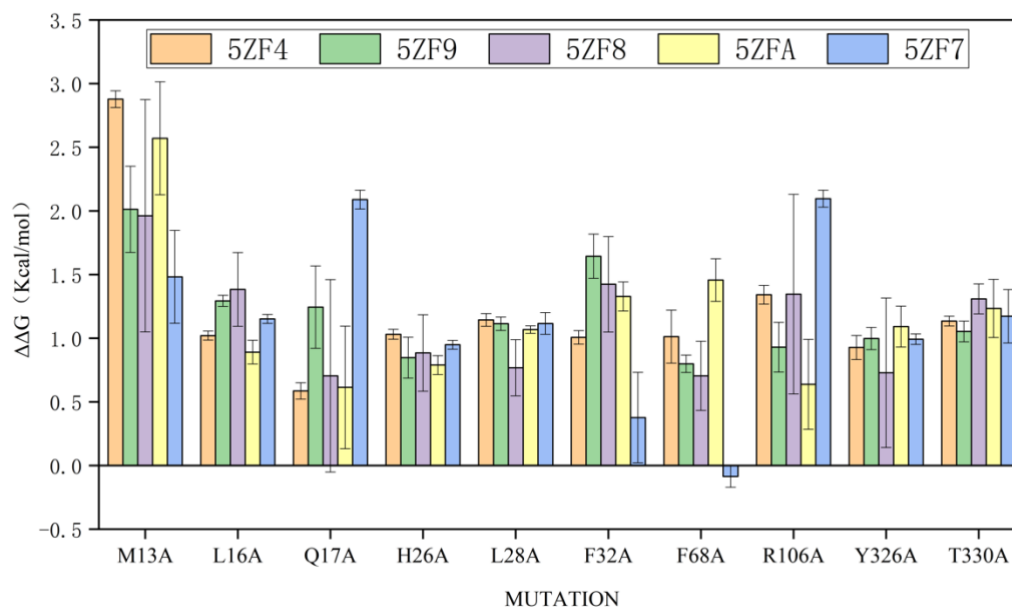


Fig5. Contribution of different residues to binding free energy for each system.

### 3.4 Virtual Screen and analysis

In general, molecules with a score of less than -11.8 kcal/mol are considered to have potential for bioactivity in virtual screening. In our study, we used a slightly more stringent threshold of -12.8 kcal/mol and selected 15 molecules from the SPECS database based on this criterion (Table S18).

To better understand the binding mechanisms and interactions of these molecules, we used RDKit to calculate their similarity to the molecules in the crystal structures (Fig. S18). Although the molecules we identified from the screening were structurally dissimilar to those in the crystal structures, they all had longer chains in terms of conformation, which is consistent with the long, narrow binding pocket of HsDHODH. This pocket can accommodate a longer chain molecule that forms stable interactions with residues in the vicinity of the pocket.

We performed MD simulations for all 15 molecules and calculated the RMSD of the ligands to ensure that all these molecules were moving within the pocket. (Fig. S2-S16) Meanwhile, ASGBIE\_ESS was also used to calculate the free energy of binding for each complex system. (Table S3-S17) We specifically analyzed the interactions of the molecule AK-968/15360669, which had the best calculation results (Fig. 5a). As shown, the ligand forms stable hydrophobic interactions with seven residues surrounding the pocket, and also forms a stable hydrogen bonding interaction with Q17 at the mouth of the pocket (Fig. 5b). We applied the same approach to analyze the residues around the pockets of the other 14 systems and found that molecules that had better predicted biological activity tended to bind more strongly to the surrounding residues. Moreover, ligands that formed stable hydrogen bonds with Q17 (e.g., AK-968/15360669, AK-

968/15360709, and AG-690/34650025) could significantly enhance their binding capacity.

In summary, our study provides insights into the binding mechanisms and interactions of molecules that have potential for bioactivity against HsDHODH. The results of our virtual screening and molecular dynamics simulations could pave the way for the development of new drug candidates targeting this enzyme.

Table2 Calculation of the ASGBIE\_ESS for the fifteen screened to molecules.

Ligand	$\Delta\Delta H$	$-T\Delta\Delta S$	$\Delta\Delta G_{cal}$
AK-968/15360669	32.3507	-4.8411	27.5096
AK-968/15360709	30.8862	-4.652	26.2342
AG-690/34650025	29.1019	-4.7171	24.3848
AG-690/11662014	28.3759	-4.3638	24.0121
AG-219/37264007	27.777	-4.1799	23.5971
AK-968/15360707	26.2914	-5.1976	21.0938
AN-329/40901050	25.1844	-4.5887	20.5957
AN-979/14070005	25.1702	-4.77	20.4002
AG-664/32343025	25.4249	-5.9198	19.5051
AK-968/15363686	23.7571	-5.4112	18.3459
AF-399/12154212	23.4779	-5.3353	18.1426
AK-918/41675822	22.8067	-5.6289	17.1778
AG-690/34647050	19.4235	-4.7101	14.7134
AM-900/40673677	21.0096	-6.3968	14.6128
AS-871/42600786	18.0796	-3.4912	14.5884

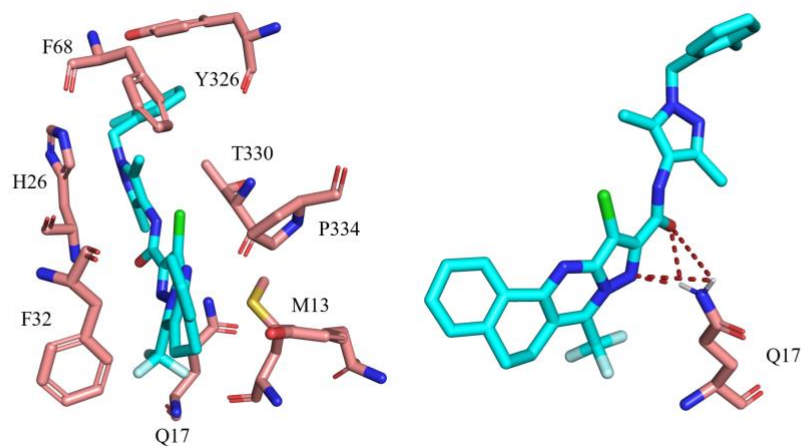


Fig6. AK-968/15360669 binds to the receptor protein.(a) AK-968/15360669 with residues in the periphery of the binding pocket. (b) AK-968/15360669 forms a hydrogen bonding interaction with Q17. Hydrogen bonds are shown as red dashed lines.

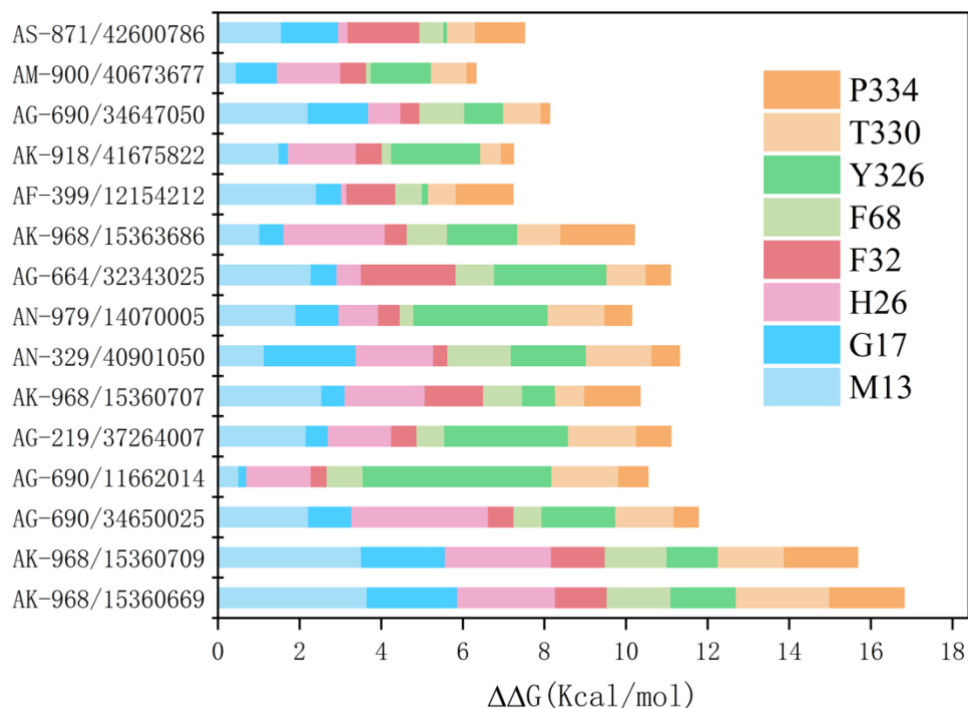


Fig7. Contribution of the energy of the residues around the binding pocket.

#### 4.CONCLUSION

Here, we investigate a novel sampling method suitable for calculating binding free energies and analyze the mode of action of ascofuranone derivatives binding to HsDHODH, which is associated with cancer, tumors, etc., using this method. Our results demonstrate that combining this new sampling method with ASGBIE provides a more accurate description of protein-ligand interactions. Furthermore, we conducted a virtual screening of this target to identify a series of compounds with entirely new backbones. These molecules contain numerous halogenated elements that could serve as novel lead compounds and be developed into a range of valuable HsDHODH inhibitors.

## 4.REFERENCE

1. Barnes, T., et al., *Regional mapping of the gene encoding dihydroorotate dehydrogenase, an enzyme involved in UMP synthesis, electron transport, and superoxide generation, to human chromosome region 16q22*. Somatic cell and molecular genetics, 1993. **19**(4): p. 405-411.
2. Evans, D.R. and H.I. Guy, *Mammalian pyrimidine biosynthesis: fresh insights into an ancient pathway*. J Biol Chem, 2004. **279**(32): p. 33035-8.
3. Peters, G.J., et al., *Inhibition of pyrimidine de novo synthesis by DUP-785 (NSC 368390)*. Invest New Drugs, 1987. **5**(3): p. 235-44.
4. McLean, J.E., et al., *Multiple inhibitor analysis of the brequinar and leflunomide binding sites on human dihydroorotate dehydrogenase*. Biochemistry, 2001. **40**(7): p. 2194-200.
5. Zhou, J., et al., *ASLAN003, a potent dihydroorotate dehydrogenase inhibitor for differentiation of acute myeloid leukemia*. Haematologica, 2020. **105**(9): p. 2286-2297.
6. Lucas-Hourani, M., et al., *Inhibition of pyrimidine biosynthesis pathway suppresses viral growth through innate immunity*. PLoS pathogens, 2013. **9**(10): p. e1003678.
7. Spina, R., et al., *DHODH inhibition impedes glioma stem cell proliferation, induces DNA damage, and prolongs survival in orthotopic glioblastoma xenografts*. Oncogene, 2022. **41**(50): p. 5361-5372.
8. Russo, T.A., et al., *Repurposed dihydroorotate dehydrogenase inhibitors with efficacy against drug-resistant *Acinetobacter baumannii**. Proceedings of the National Academy of Sciences, 2022. **119**(51): p. e2213116119.
9. Wang, R., et al., *Molecular Mechanism of Selective Binding of NMS-P118 to PARP-1 and PARP-2: A Computational Perspective*. Frontiers in Molecular Biosciences, 2020. **7**.
10. Hou, T., et al., *Assessing the Performance of the MM/PBSA and MM/GBSA Methods. 1. The Accuracy of Binding Free Energy Calculations Based on Molecular Dynamics Simulations*. Journal of Chemical Information and Modeling, 2011. **51**(1): p. 69-82.
11. Bash, P.A., M.J. Field, and M. Karplus, *Free energy perturbation method for chemical reactions in the condensed phase: a dynamic approach based on a combined quantum and molecular mechanics potential*. Journal of the American Chemical Society, 1987. **109**(26): p. 8092-8094.
12. Rao, S.N., et al., *Free energy perturbation calculations on binding and catalysis after mutating Asn 155 in subtilisin*. Nature, 1987. **328**(6130): p. 551-554.
13. Kollman, P., *Free energy calculations: Applications to chemical and biochemical phenomena*. Chemical Reviews, 1993. **93**(7): p. 2395-2417.
14. Beveridge, D.L. and F.M. DiCapua, *Free energy via molecular simulation: applications to chemical and biomolecular systems*. Annu Rev Biophys Biophys Chem, 1989. **18**: p. 431-92.
15. Zacharias, M., T.P. Straatsma, and J.A. McCammon, *Separation-shifted scaling, a new scaling method for Lennard-Jones interactions in thermodynamic integration*. The Journal of Chemical Physics, 1994. **100**(12): p. 9025-9031.

16. Massova, I. and P.A. Kollman, *Computational Alanine Scanning To Probe Protein–Protein Interactions: A Novel Approach To Evaluate Binding Free Energies*. Journal of the American Chemical Society, 1999. **121**: p. 8133-8143.
17. Massova, I. and P.A. Kollman, *Combined molecular mechanical and continuum solvent approach (MM-PBSA/GBSA) to predict ligand binding*. Perspectives in drug discovery and design, 2000. **18**(1): p. 113-135.
18. Moreira, I.S., P.A. Fernandes, and M.J. Ramos, *Computational alanine scanning mutagenesis—an improved methodological approach*. Journal of Computational Chemistry, 2007. **28**(3): p. 644-654.
19. Sun, H., et al., *Assessing the performance of MM/PBSA and MM/GBSA methods. 5. Improved docking performance using high solute dielectric constant MM/GBSA and MM/PBSA rescoring*. Physical Chemistry Chemical Physics, 2014. **16**(40): p. 22035-22045.
20. Sun, H., et al., *Assessing the performance of MM/PBSA and MM/GBSA methods. 7. Entropy effects on the performance of end-point binding free energy calculation approaches*. Physical Chemistry Chemical Physics, 2018. **20**(21): p. 14450-14460.
21. Duan, L., X. Liu, and J.Z. Zhang, *Interaction entropy: a new paradigm for highly efficient and reliable computation of protein–ligand binding free energy*. Journal of the American Chemical Society, 2016. **138**(17): p. 5722-5728.
22. Cong, Y., et al., *Trypsin–ligand binding affinities calculated using an effective interaction entropy method under polarized force field*. Scientific reports, 2017. **7**(1): p. 1-12.
23. Burgoyne, N.J. and R.M. Jackson, *Predicting protein interaction sites: binding hot-spots in protein–protein and protein–ligand interfaces*. Bioinformatics, 2006. **22**(11): p. 1335-1342.
24. Barillari, C., G. Marcou, and D. Rognan, *Hot-spots-guided receptor-based pharmacophores (HS-Pharm): a knowledge-based approach to identify ligand-anchoring atoms in protein cavities and prioritize structure-based pharmacophores*. Journal of chemical information and modeling, 2008. **48**(7): p. 1396-1410.
25. Cheung, L.S.-L., et al., *A hot-spot motif characterizes the interface between a designed ankyrin-repeat protein and its target ligand*. Biophysical journal, 2012. **102**(3): p. 407-416.
26. Bauman, J.D., J.J.E. Harrison, and E. Arnold, *Rapid experimental SAD phasing and hot-spot identification with halogenated fragments*. IUCrJ, 2016. **3**(1): p. 51-60.
27. Yan, Y., et al., *Interaction entropy for computational alanine scanning*. Journal of Chemical Information and Modeling, 2017. **57**(5): p. 1112-1122.
28. Qiu, L., et al., *Interaction entropy for computational alanine scanning in protein–protein binding*. Wiley Interdisciplinary Reviews: Computational Molecular Science, 2018. **8**(2): p. e1342.
29. Gohlke, H., M. Hendlich, and G. Klebe, *Predicting binding modes, binding affinities and hot spots' for protein–ligand complexes using a knowledge-based scoring function*. Perspectives in Drug Discovery and Design, 2000. **20**(1): p. 115-144.
30. Berman, H.M., et al., *The Protein Data Bank*. Nucleic Acids Research, 2000. **28**(1): p. 235-242.



31. Bietz, S., et al., *Protoss: a holistic approach to predict tautomers and protonation states in protein-ligand complexes*. Journal of Cheminformatics, 2014. **6**(1): p. 12.
32. Lippert, T. and M. Rarey, *Fast automated placement of polar hydrogen atoms in protein-ligand complexes*. Journal of Cheminformatics, 2009. **1**(1): p. 13.
33. Maier, J.A., et al., *ff14SB: improving the accuracy of protein side chain and backbone parameters from ff99SB*. Journal of chemical theory and computation, 2015. **11**(8): p. 3696-3713.
34. Wang, J., et al., *Development and testing of a general amber force field*. Journal of computational chemistry, 2004. **25**(9): p. 1157-1174.
35. Jorgensen, W.L., et al., *Comparison of simple potential functions for simulating liquid water*. The Journal of chemical physics, 1983. **79**(2): p. 926-935.
36. Halgren, T.A., et al., *Glide: A New Approach for Rapid, Accurate Docking and Scoring. 2. Enrichment Factors in Database Screening*. Journal of Medicinal Chemistry, 2004. **47**(7): p. 1750-1759.